

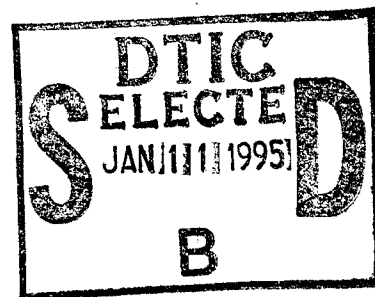
NATIONAL AIR INTELLIGENCE CENTER



METHOD OF SPACE-TIME SEQUENCE TRANSFORM USED TO MEASURE
ACOUSTO-OPTIC DEFLECTION AND MODULATION

by

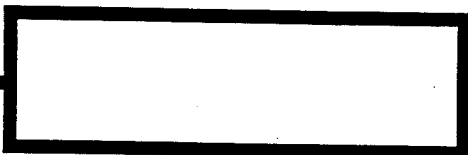
Feng Bihua, Pen Zhiping, Huang Zonghua



19950109 122

19950109 122

Approved for public release;
Distribution unlimited.



HUMAN TRANSLATION

NAIC-ID(RS)T-0384-94 16 December 1994

MICROFICHE NR: 946000571

METHOD OF SPACE-TIME SEQUENCE TRANSFORM USED TO
MEASURE ACOUSTO-OPTIC DEFLECTION AND MODULATION

By: Feng Bihua, Pen Zhiping, Huang Zonghua

English pages: 9

Source: Nanjing Daxue Xuebao, Vol. 27, Nr. 3, July 1991;
pp. 599-603

Country of origin: China

Translated by: Leo Kanner Associates
F33657-88-D-2188

Quality Control: Nancy L. Burns

Requester: NAIC/TATA/J.M. Finley

Approved for public release; Distribution unlimited.

THIS TRANSLATION IS A RENDITION OF THE ORIGINAL
FOREIGN TEXT WITHOUT ANY ANALYTICAL OR EDITO-
RIAL COMMENT STATEMENTS OR THEORIES ADVOC-
ATED OR IMPLIED ARE THOSE OF THE SOURCE AND
DO NOT NECESSARILY REFLECT THE POSITION OR
OPINION OF THE NATIONAL AIR INTELLIGENCE CENTER.

PREPARED BY:

TRANSLATION SERVICES
NATIONAL AIR INTELLIGENCE CENTER
WPAFB, OHIO

GRAPHICS DISCLAIMER

All figures, graphics, tables, equations, etc. merged into this translation were extracted from the best quality copy available.

Accession For	
NTIS GRA&I	<input checked="checked" type="checkbox"/>
DTIC TAB	<input type="checkbox"/>
Unannounced	<input type="checkbox"/>
Justification	
By	
Distribution/	
Availability Codes	
Dist	Avail and/or Special
A-1	

METHOD OF SPACE-TIME SEQUENCE TRANSFORM USED TO MEASURE ACOUSTO-OPTIC DEFLECTION AND MODULATION

Feng Bihua, Pen Zhiping, and Huang Zonghua; all of Department of
Physics, Nanjing University

Abstract

This paper describes that the method of spatial sequence to be transformed into time sequence is used to measure the complete picture of the α -f curve that is of realtime, series and stability. This method is also used to measure dynamical process of variation in distribution of relative intensity of light, which varies with plate current as Bragg's diffraction.

The experimental results coincide with the theory of acous-to-optics interaction.

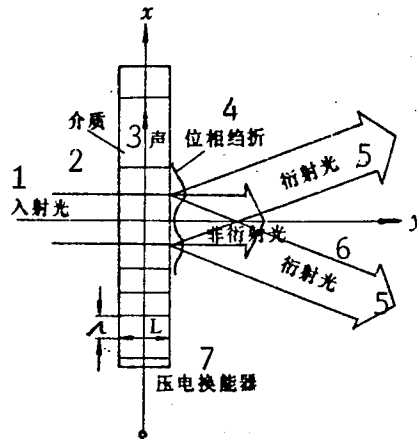
Keywords: Deflection of acousto-optic, modulation of acousto-optic, spatial-time sequence transform

I. Fundamental Principle

When a plane light wave passes through a medium with thickness L , and encounters with an acoustic wave, as shown in Fig. 1, the change in phase displacement is

$$\Delta\phi(x) = n(x)k_0L = \\ nk_0L + uk_0L\sin(kx - \Omega t)$$

In the equation, k_0 is the number of optical waves in vacuo; k is the number of acoustic waves in the medium; and Ω is the acoustic angular frequency. μ is the amplitude of refractivity change.



KEY: 1. Incident light
 2. Medium 3. Sound
 4. Deflection of displacement phase
 5. Diffractive light
 6. Nondiffractive light
 7. Piezoelectric transducer

The acousto-optic interaction can be summarized as a collisional process between phonons and photons; the collisional process should obey the law of conservation of momentum and conservation of energy. With upper frequency displacement

$\vec{k}_i + \vec{k} = \vec{k}_{d+}$ (conservation of momentum) and $\vec{k}_i - \vec{k} = \vec{k}_{d-}$ (conservation of momentum)

$$\omega_i + \Omega = \omega_d$$

(conservation of energy)

$$\omega_i - \Omega = \omega_d$$

(conservation of momentum)

The subscript d indicates the amount of deflection; when the triangle is closed, because of the action of k_i , the only diffractive light \vec{d}_{d+} (or \vec{k}_{d-}) is generated due to the function of \vec{K} . Meanwhile, the angle of shift $\alpha = 2\theta_s \approx \frac{\lambda}{\Lambda} = \frac{\lambda}{nv_s} f$ between order 0 and order 1

λ is the optical wavelength in the medium; Λ is the acoustic wavelength.

Raman-Nath deflection corresponds to continuous interaction between an incident light and several phonons; there is

$$\begin{aligned}\vec{k}_d^{(m)} &= k_i + m\vec{k} \\ \omega_d^{(m)} &= \omega_i + m\Omega\end{aligned}$$

In the equation of m-order diffraction efficiency $\eta = \frac{I_m}{I_i} = J_m^2[2\zeta L \sin\{\frac{kL}{2\cos\theta_i} - (\sin\theta_i - m\frac{K}{k})\}]$ I_i is the incident light intensity

$$\zeta = \frac{1}{4} \frac{\epsilon_i k}{\epsilon_0 \cos\theta_i}$$

In the equation of the Bragg diffraction efficiency $\eta = \frac{I_1}{I_i} = (\zeta L)^2 \sin^2(\sigma L)$, $\sigma^2 = (\frac{\beta_1}{2})^2 + \zeta^2$. During strict Bragg diffraction $\sigma = \zeta$, then $\eta = \sin^2[\frac{\pi}{\sqrt{2}\lambda_0 \cos\theta_i} \sqrt{M_2 P_a \frac{L}{H}}]$. At that time, the diffraction light intensities of order 0 and order 1 are, respectively,

$$I_0 = I_i \cos^2(\zeta L) \quad I_1 = I_i \sin^2(\zeta L) \quad \text{其中 } \zeta L = \frac{\pi}{\sqrt{2}\lambda_0 \cos\theta_i} \sqrt{M_2 P_a \frac{L}{H}} = K\sqrt{P_a}$$

In the equation

$$M_2 = \frac{n^6 P^2}{\rho v_s^3} \quad \text{acousto-optic quality factor}$$

$$P_a = \frac{1}{2} E |s|^2 v_s L H \quad \text{acoustic power}$$

L/H is the length-to-width ratio of the transducer; E is Young's modulus.

II. Measurement Method and Result

Fig. 2 shows the measurement installation used in the experiment.

In the figure, the dashed square shows a new method developed by the authors for using fiber optics techniques to enable the real-time display of the relative light intensity distribution curve. When the diffraction fringes are illuminated onto the light entrance window, through a space-time sequence

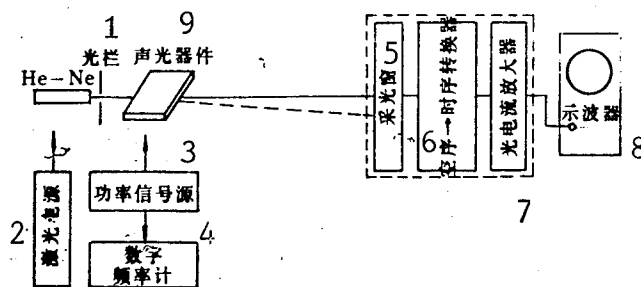


Fig. 2 Arrangement of experimental apparatus

KEY: 1. Diaphragm 2. Laser power source 3. Power signal source
4. Digital frequency meter 5. Light entrance window 6. Space
sequence to time sequence transform device 7. Amplifier for optical-electric
current 8. Oscillograph 9. Acous-
to-optical device

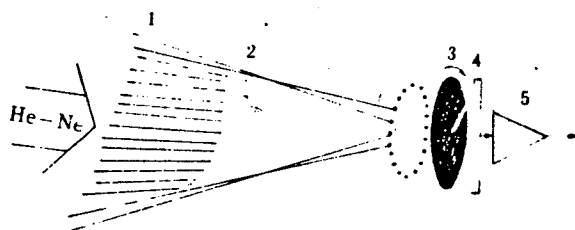


Fig. 3. Space-time sequence transform device

transform device, the relative light intensities are converted into a time-varying function according to variation in spatial position, and changes into optical-electric current for linear relationship with the light intensity. After appropriate amplification, the optical-electric current is fed to the Y-axis of the oscillograph for display and measurement. Since the method adopts high-speed optical scanning of 50 times per second (that is, a special distribution diagram of 50 frames of light intensity can be displayed per second), and at the same time a synchronous pulse and sweep line marker generator is placed. Therefore, a conventional model oscillograph can have provide real-time observation and stability with the distribution curve of relative light intensity with clear and continuous diffraction

fringes. This is very beneficial when it is required to measure relative variations of various diffraction-order light intensities in measuring diffraction fringes on a dynamic basis. However, for a conventional microcomputer collecting system, one scanning requires about 2min. This is difficult to achieve real-time display of light intensity distribution curves. The key to having real-time display method of relative light intensity distribution curves is a space-time sequence transform device. The authors carried out the method by adopting fiber optics technology. A block diagram of the space-time sequence transform device is shown in Fig. 3.

In Fig. 3, 1 is the light entrance window; 2 is the optical fiber; 3 is the diaphragm; 4 is the optical-electric element; and 5 is the amplifier for the optical-electric element. When the diffraction fringes are illuminated onto the line terminals (that is, the light entrance window) of the optical fiber, the light intensity distribution sequence is distributed on the circumference of the circular terminals of the optical fiber through its arrangement. By passing through a rotating diaphragm, the light intensity distributed on the circular circumference is scanned; this corresponds to light intensity scanning as distributed on the line terminals. Thus, the transform from "line" to "circle" is achieved; thus, high-speed can be accomplished. At the same time, the space-time sequence transform is carried out. The triggering arrangement of the oscillograph is of the internal type; moreover, the marked signal indicating the scanning of the origin and endpoint of the light entrance window is also used as the synchronous pulse. When adjusting the oscillograph so that the spacing between two scanning marked lines is a certain value (86mm), at this time the distance between two points along the X-direction of the oscillograph is the distance of these two points on the light entrance window, or as the relationship of $_$ correspondence.

During the experiments, adjust the included angle (incident angle) between the incident light and the acousto-optic device by

slightly rotating it left or right, so that Raman-Nath diffraction and Bragg diffraction, respectively, can appear. When adjusting the Bragg diffraction, the diffraction fringes are projected onto the light entrance window; thus, the whole picture of light intensity distribution curve can be observed on the oscillograph. As shown in Fig. 4, the five small peak values from left to right correspond to order-1 diffractive light intensity at acoustic frequencies of 50MHz, 74MHz, 98MHz, 120MHz, and 150MHz. The highest peak at the center is order-0 light intensity. This is a picture obtained through five light exposures and then one image development and fixation. From the curves in Fig. 4, the authors measured the distances of order-0 and order-1, then they measured the distance between the acousto-optical sample and the light entrance window. Thus, the various α values can be computed, thus obtaining the α -f curve as shown in Fig. 5.

In addition, the authors measured the acousto-optical modulation curve by using the space-time sequence transform method; the experimental set-up is the same as that of Fig. 1. Fig. 6 shows the acousto-optical modulation curve when the fixed acoustic frequency $f=8.3\text{MHz}$. This curve indicates the dynamic process that the relative light intensity distribution in the case of Bragg diffraction varies with the plate current of the ultrasonic power signal source. The three peak values from left to right correspond to diffractive light intensity of order-0, order-1, and order-2, respectively. From Fig. 6 we see that the maximum value of I_1 is still smaller than the maximum value of I_0 ; this is because the experimental conditions do not strictly satisfy the Bragg condition; however, the order-2 diffractive light intensity I_2 is still smaller. This explains that the authors' experiment basically still matches with the Bragg

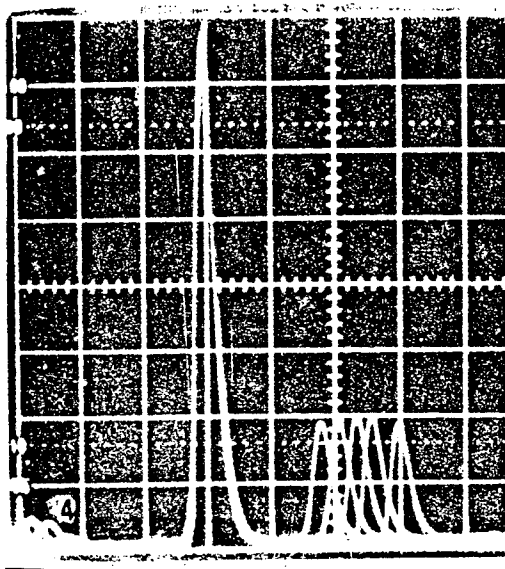


Fig.4 α - f (acoustic frequency) multiexposure photo

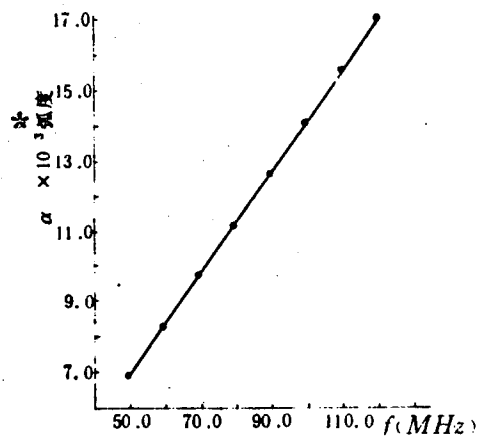


Fig.5 α - f curve

KEY: * - radian

diffraction conditions. At the like-numbered locations, these correspond to various orders of diffractive light intensity at the same ultrasonic power value. The numbers 1 through 5 indicate the gradual increasing electric power of the ultrasonic-powered signal source of the driving acousto-optical device; in other words, the plate current i_a increases gradually. Although researchers find it difficult to measure the ultrasonic power, however, when the electric power of the ultrasonic-powered signal source is at a certain amount (i_a is at a certain value), the ultrasonic power is also at a certain value.

In actual measurements, the authors fixed the acoustic frequency $f=83\text{MHz}$ and selected ten gradually increasing electric power values based on numerical sequence. This was done by changing the plate current i_a of the ultrasonic-powered signal source. Thus, the relationship curve indicating the relative light intensity I is proportional to i_a . We can see that at the beginning stage, as i_a increases, I_1 also increases with faster rate. After i_a is greater than a certain value, I_1 gradually tends to saturation, and beginning the appearance of a new round

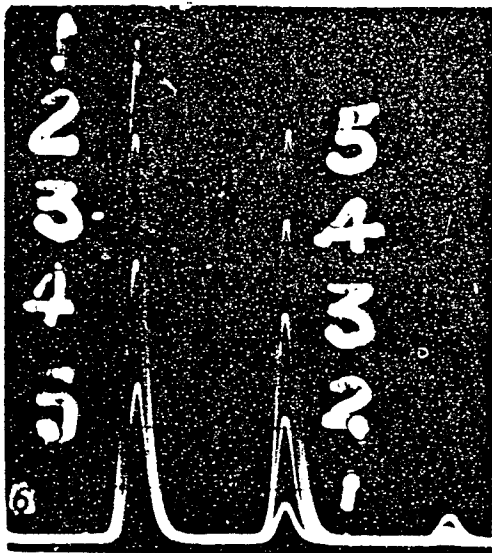


Fig.6 Light intensity of Bragg diffraction at different acoustic power

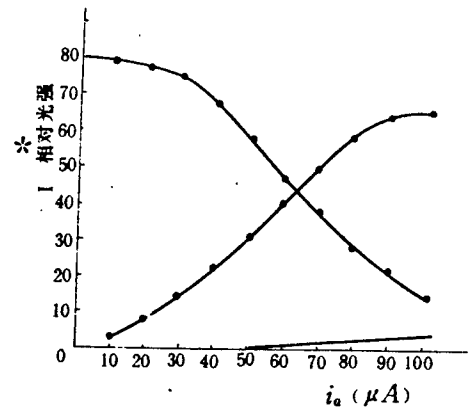


Fig.7 $I \sim i_a$ (plate current) curve

KEY: * - Relative light intensity

energy exchange between I_0 and I_1 . The experimental results are in agreement with theory. If i_a continues to increase, so that $\zeta = \pi$, $\eta_N = 0$, $I_1 = 0$. In other words, the energy relationship between I_0 and I_1 will be restored to the state of the absence of an ultrasonic field. Because of limited power of the ultrasonic signal generator that the authors used, the phenomena of this portion remain unobserved.

The paper was received for publication on July 27, 1989.

REFERENCES

- 1 Korpel A. Acousto-Optics Applied Solid State Science. 1972;3:72-175
2. Xu Jieping, Shengguang qijian di yuanli, sheji he yingyong
[Principle, Design and Applications of Acousto-optical
Devices], Science Publishing House, 1982.
3. Jia Zhifu, Huang Zonghua, et al., Shengxue celiang jiangyi
[Lecture Notes on Acoustic Measurements], Defense Industry
Publishing House, 1990.

DISTRIBUTION LIST

DISTRIBUTION DIRECT TO RECIPIENT

<u>ORGANIZATION</u>	<u>MICROFICHE</u>
B085 DIA/RTS-2FI	1
C509 BALLOC509 BALLISTIC RES LAB	1
C510 R&T LABS/AVEADCOM	1
C513 ARRADCOM	1
C535 AVRADCOM/TSARCOM	1
C539 TRASANA	1
Q592 FSTC	4
Q619 MSIC REDSTONE	1
Q008 NTIC	1
Q043 AFMIC-IS	1
E051 HQ USAF/INET	1
E404 AEDC/DOF	1
E408 AFWL	1
E410 AFDTC/IN	1
E429 SD/IND	1
P005 DOE/ISA/DDI	1
P050 CIA/OCR/ADD/SD	2
1051 AFIT/LDE	1
P090 NSA/CDB	1
2206 FSL	1

Microfiche Nbr: FTD94C000571
NAIC-ID(RS)T-0384-94